

For a wire sample, we integrate again, using Eq. (A17):

$$\bar{g} = \frac{1}{2r} \int_{-r}^r \left\{ \frac{1}{\rho_0 + K} - 2 \frac{aK}{(\rho_0 + K)^2} (r^2 - x^2) \right\} dx, \quad (\text{A18})$$

$$\bar{g} = \frac{1}{\rho_0 + K} - \frac{\pi}{4} \frac{aK}{(\rho_0 + K)^2} d. \quad (\text{A19})$$

The correction to the resistivity increase due to irradiation is, approximately,

$$\Delta\rho_c = \frac{1}{4}\pi aKd.$$

Since  $K$  is the true increase in resistivity, the desired increase in resistivity to compare with theory is

$$\rho = \rho_m (1 + \frac{1}{4}\pi ad)^{-1},$$

where  $\rho_m$  is the measured resistivity increase.

## Far Infrared Dielectric Dispersion in BaTiO<sub>3</sub>, SrTiO<sub>3</sub>, and TiO<sub>2</sub>

W. G. SPITZER, ROBERT C. MILLER, D. A. KLEINMAN, AND L. E. HOWARTH  
Bell Telephone Laboratories, Murray Hill, New Jersey

(Received January 24, 1962)

The room temperature reflectivity of BaTiO<sub>3</sub>, SrTiO<sub>3</sub>, and TiO<sub>2</sub> has been measured from 5000 to 70 cm<sup>-1</sup>. These data have been analyzed by the Kramers-Kronig method and by classical dispersion theory. All of the infrared-active fundamental vibrations allowed by crystal symmetry have been measured and characterized by their dispersion parameters. Of particular interest is the low-frequency mode which recent theories show is responsible for ferroelectricity in BaTiO<sub>3</sub> and SrTiO<sub>3</sub> and is found at 33.8 and 87.7 cm<sup>-1</sup>, respectively. The unusually large damping found for this mode can explain the observed microwave loss tangents. The strength of the mode accounts for the large values of the low-frequency dielectric constant. This mode, as well as the highest frequency mode, 510 and 546 cm<sup>-1</sup> in BaTiO<sub>3</sub> and SrTiO<sub>3</sub>, respectively, is associated with TiO<sub>6</sub> octahedra vibrations. A previously unreported mode at 183 and 178 cm<sup>-1</sup> for BaTiO<sub>3</sub> and SrTiO<sub>3</sub>, respectively, has also been found and assigned to a cation-(TiO<sub>3</sub>) vibration. In rutile, three resonances are observed for the ordinary ray and one for the extraordinary ray, as required by theory. As with the titanates, the high dielectric constant is associated with the low-frequency mode. An analysis of the strengths of all of the resonances shows that they involve reasonable effective charges for ionic crystals.

### INTRODUCTION

ONE of the most striking characteristics of the oxide ferroelectric materials,<sup>1</sup> such as the titanates and niobates, is the large value of  $\epsilon_0$  the dielectric constant in the microwave and lower-frequency parts of the electromagnetic spectrum. At temperatures in the neighborhood of the Curie point of these materials, dielectric constants of the order of  $10^4$  are observed. In contrast to these large values, the high frequency or optical dielectric constants  $\epsilon_\infty$  are below 10. These materials have not in most cases been studied in the portion of the frequency spectrum, called the *transition region*, where the dielectric constant changes from  $\epsilon_\infty$  to  $\epsilon_0$ . Considered in the present paper are two materials which in some temperature region are ferroelectric, BaTiO<sub>3</sub> and SrTiO<sub>3</sub>. Rutile,<sup>2</sup> TiO<sub>2</sub>, which is not ferroelectric but exhibits high values for  $\epsilon_0$  and has the TiO<sub>6</sub> octahedra structure in common with the titanates, was also studied. At room temperature, where these materials are investigated, BaTiO<sub>3</sub> is tetragonal and ferroelectric, SrTiO<sub>3</sub> is cubic

and paraelectric, and TiO<sub>2</sub> is tetragonal and a normal dielectric.

On the microwave side of the transition region, the two highest frequencies at which single crystals of BaTiO<sub>3</sub> have been measured, 0.8 cm<sup>-1</sup> (24 kMc/sec)<sup>3</sup> and 1.87 cm<sup>-1</sup> (56 kMc/sec),<sup>4</sup> both indicated a room temperature dielectric constant for electric fields perpendicular to the optic axis  $\epsilon_{11}$  of 2000. (For convenience, all frequencies will be given in cm<sup>-1</sup>.) The loss tangent was reported to be about 0.1. Measurements on single-crystal SrTiO<sub>3</sub> at frequencies up to 1.2 cm<sup>-1</sup> (36 kMc/sec)<sup>5</sup> did not show any dispersion in the dielectric constant  $\epsilon$  which is<sup>6</sup> about 310 at room temperature. The loss tangent at room temperature is  $1.5 \times 10^{-3}$  at 0.73 cm<sup>-1</sup> (22 kMc/sec).<sup>5</sup>

Both SrTiO<sub>3</sub> and BaTiO<sub>3</sub> have been studied by Last<sup>7</sup> from 1000 cm<sup>-1</sup> to about 300 cm<sup>-1</sup>. Last claimed to have observed two of the three predicted optically active normal modes. The two resonances reported were as-

<sup>3</sup> T. S. Benedict and J. L. Durand, Phys. Rev. **109**, 1091 (1958).

<sup>4</sup> R. F. Trambarulo (quoted in reference 3).

<sup>5</sup> G. Rupprecht, R. O. Bell, and B. D. Silverman, Phys. Rev. **123**, 97 (1961).

<sup>6</sup> A. Linz, Jr., Phys. Rev. **91**, 753 (1953); G. Rupprecht (unpublished data).

<sup>7</sup> J. T. Last, Phys. Rev. **105**, 1740 (1957).

<sup>1</sup> For a general review on the subject of ferroelectricity the reader is referred to W. Känzig, in *Solid-State Physics*, edited by F. Seitz and D. Turnbull (Academic Press Inc., New York, 1957), Vol. IV.

<sup>2</sup> For a general review article on TiO<sub>2</sub>, the reader is referred to F. A. Grant, Revs. Modern Phys. **31**, 646 (1959).

signed to two  $\text{TiO}_6$  octahedra normal modes, while a third resonance, which was described as a cation—( $\text{TiO}_3$ ) mode, was estimated to be at a wavelength beyond the range of the equipment. These infrared data seemed to indicate (to the present authors) that the transition region was below  $350\text{ cm}^{-1}$ . Therefore, the conclusion drawn from the infrared and microwave data was that the transition region for  $\text{BaTiO}_3$  and  $\text{SrTiO}_3$  must be somewhere between about  $350$  and  $1\text{ cm}^{-1}$ . The results of the present study and their interpretation differ in several important respects from those of Last.

While investigating the two titanates, it became clear that  $\text{TiO}_2$  single crystals should also be studied. The fact that rutile has the  $\text{TiO}_6$  octahedra but lacks the cation- $\text{TiO}_3$  structure is most helpful in characterizing the modes in the materials studied. Liebisch and Rubens,<sup>8</sup> in 1921, obtained reflectivity data for rutile from the near infrared to  $33\text{ cm}^{-1}$  ( $300\ \mu$ ). These measurements were treated by von Hippel *et al.*<sup>9</sup> in terms of classical dispersion theory. The analysis, which did not yield an accurate fit to the data, indicated that the response of large strength, i.e., the normal mode responsible for most of the low-frequency dielectric constant, was located at about  $200\text{ cm}^{-1}$ . Rutile has been remeasured in the course of the present study, and significant differences are observed between the present results and those reported by Liebisch and Rubens.

There are a number of important reasons for studying materials with high dielectric constant in some detail. The manner in which  $\epsilon$  changes from  $\epsilon_\infty$  to  $\epsilon_0$  is of fundamental interest. The static theories of the thermodynamic behavior of  $\text{BaTiO}_3$  given by Devonshire<sup>10</sup> and Slater<sup>11</sup> cannot predict how this will take place. On the other hand, recent theories by Anderson<sup>12</sup> and by Cochran<sup>13</sup> have emphasized the essential role played by a single optical mode of vibration in the ferroelectric transition. These theories would suggest that the transition from  $\epsilon_\infty$  to  $\epsilon_0$  should obey classical dispersion theory for a very strong resonance lying in the far infrared or millimeter region. Furthermore, it may be possible to correlate the damping of this resonance with the loss tangents observed in the microwave region.<sup>9</sup> If the dispersion mechanism is indicated, it will be of interest to ascertain if the large change in dielectric constant ( $\Delta\epsilon$  of the order of hundreds or thousands) can be described quantitatively in terms of classical dispersion theory which has been applied with much success to

dispersions where the dielectric constant changes by the order of unity.<sup>14</sup>

After the present data had been accumulated, it came to the attention of the authors that an independent far infrared reflectivity measurement of  $\text{SrTiO}_3$  by Barker and Tinkham<sup>15</sup> (BT) was in progress and nearing completion. The present authors have had the benefit of a preprint of the paper describing this work, so that frequent reference to it is made in the text. The BT reflectivity data were analyzed in terms of the real and imaginary parts of the dielectric constant which showed that the transition in dielectric constant is resonant in form and not a relaxation. BT found two of the three predicted<sup>7</sup> resonances, one at  $550\text{ cm}^{-1}$  (also reported by Last) and one of large strength (previously not reported) at  $100\text{ cm}^{-1}$ , both at room temperature. Measurements at  $93^\circ\text{K}$  showed that the resonance of large strength moves to lower frequency ( $40\text{ cm}^{-1}$ ) with decreasing temperature. Some aspects of the results were interpreted in terms of a recent theory which relates certain lattice vibrations to ferroelectricity.<sup>13</sup> The present results and conclusions on  $\text{SrTiO}_3$  are, in general, in qualitative agreement with those of BT. However, there are a few significant differences between the two studies.

In the present experiments, infrared reflectivity measurements have been obtained for  $\text{SrTiO}_3$ ,  $\text{BaTiO}_3$ , and  $\text{TiO}_2$  from  $5000$  to about  $70\text{ cm}^{-1}$ . These reflectivity measurements have been subjected to Kramers-Kronig (K-K) analyses for the real and imaginary parts of the dielectric constant. Attempts were made to fit the reflectivity data for each of the three materials with classical dispersion theory starting with dispersion parameters calculated from the K-K analyses. In the case of  $\text{BaTiO}_3$ , thin sample transmission measurements were also made, and the experimental transmission is compared with that calculated from the K-K data. Loss tangents in the microwave region around  $1\text{ cm}^{-1}$  have also been estimated. The assignment of the various resonances observed to normal mode lattice vibrations is discussed. A discussion comparing the present results with those of Last, BT, and the much earlier work on  $\text{TiO}_2$ , as well as their interpretation in terms of the limited theory currently available, is also given.

#### SAMPLE PREPARATION

Undoped single crystals of  $\text{BaTiO}_3$  were grown by the Remeika method.<sup>16</sup> Clear crystal plates with good clean surfaces were selected and etched in concentrated  $\text{H}_3\text{PO}_4$  at  $155^\circ\text{C}$  sufficiently long to remove an anomalous surface layer of about  $3 \times 10^{-3}\text{ cm}$  in thickness.<sup>17</sup> The final

<sup>8</sup> T. Liebisch and H. Rubens, Sitzber. preuss. Akad. Wiss., Physik.-math Kl. 8, 211 (1921).

<sup>9</sup> A. von Hippel, R. G. Breckenridge, F. G. Chesley, and L. Tisza, Ind. Eng. Chem. 38, 1097 (1946).

<sup>10</sup> A. F. Devonshire, Phil. Mag. 40, 1040 (1949); 42, 1065 (1951).

<sup>11</sup> J. C. Slater, Phys. Rev. 78, 748 (1950).

<sup>12</sup> P. Anderson, in *Fizika dielektrikov*, edited by G. I. Skanavi (Akademichâ Nauk S.S.S.R. Fizicheskii Inst. im P. N. Lebedeva, Moscow, 1960).

<sup>13</sup> W. Cochran, *Advances in Physics*, edited by N. F. Mott (Taylor and Frances, Ltd., London, 1960), Vol. 9, p. 387.

<sup>14</sup> W. G. Spitzer and D. A. Kleinman, Phys. Rev. 121, 1324 (1961).

<sup>15</sup> A. S. Barker and M. Tinkham, Phys. Rev. 125, 1529 (1962).

<sup>16</sup> J. P. Remeika, J. Am. Chem. Soc. 76, 940 (1954).

<sup>17</sup> C. F. Pulvari, Proceedings of the Spec. Tech. Conference, Solid-State Dielectric and Magnetic Devices, April, 1957, Catholic University of America, Washington, D. C. (unpublished), paper 4.

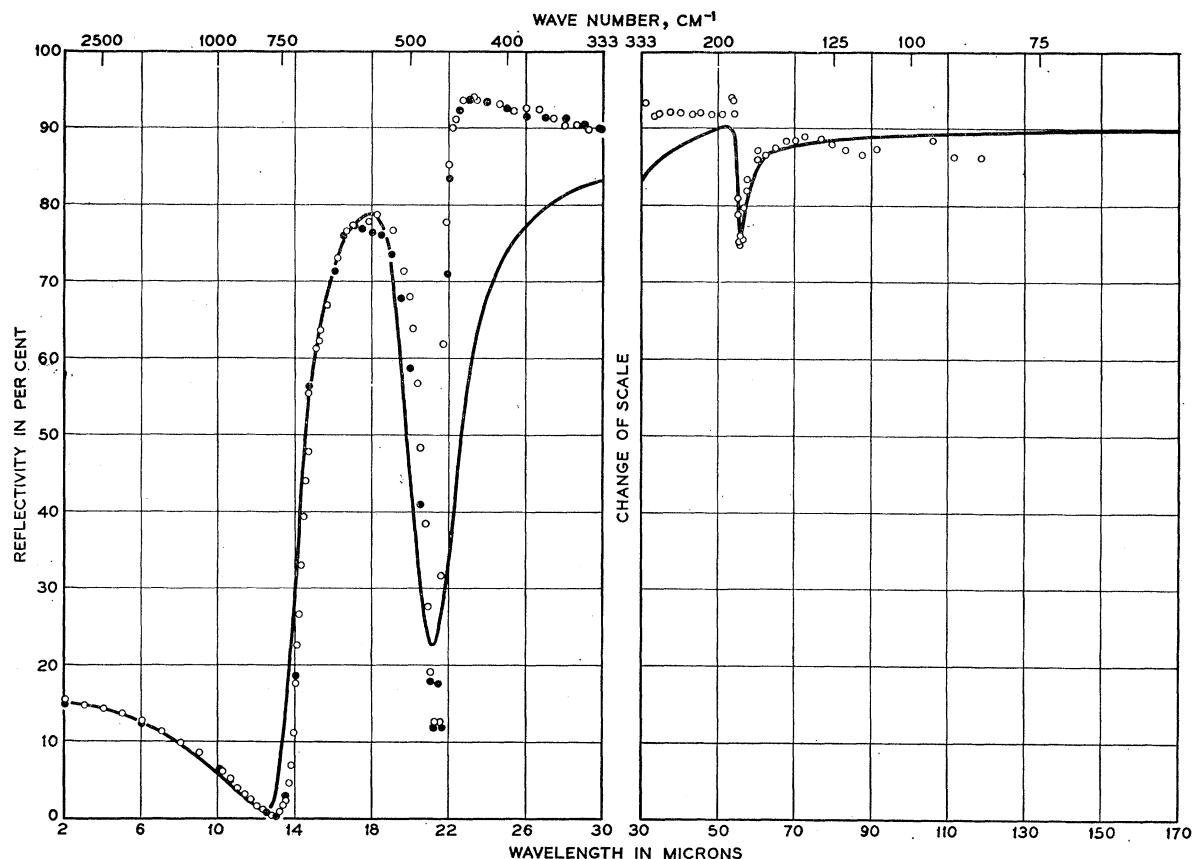


FIG. 1. Reflectivity of  $\text{BaTiO}_3$  for both the ordinary ray (open circles) and extraordinary ray (dots). The curve was calculated by using dispersion theory.

sample thicknesses were of the order  $10^{-2}$  cm. After etching they were converted to  $c$ -domain plates by dc poling in water. The samples were then examined with a polarizing microscope, and only those which were entirely  $c$  domained, i.e., the optic axis everywhere normal to the large area surfaces, were selected for measurement. Since the surfaces as grown were of

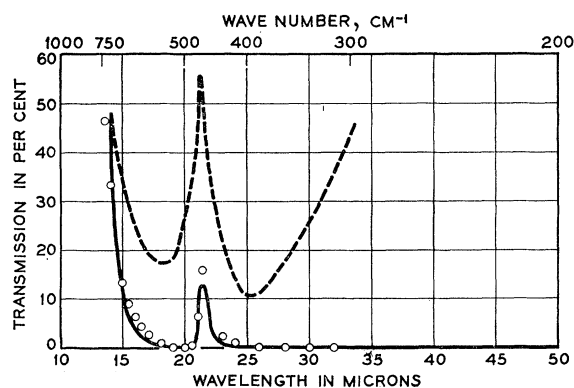


FIG. 2. The measured transmission of a  $(5.0 \pm 0.5) \mu$  thick  $\text{BaTiO}_3$  sample is given by the open circles. The solid curve is a calculated curve using the optical constants from the Kramers-Kronig analysis of the data in Fig. 1. The dashed curve gives the transmission of a  $\text{KBr-BaTiO}_3$  powder pellet.

sufficiently good optical quality to permit infrared measurements, no attempt was made to polish the samples. For the far-infrared region it was necessary to butt two samples together to obtain a sufficiently large area, approximately  $1 \text{ cm}^2$ , so that the signal-to-noise level would be reasonable. In order to measure samples with the electric field parallel to the optic axis, it was necessary to introduce  $a$  domains into the crystal, i.e., regions in which the optic axis, and hence the polarization direction, is parallel to the plane of the surface. The method described by Fang<sup>18</sup> was used to introduce  $a$  domains, however, it was estimated that only about 50% of the crystal volume could be converted to the desired orientation. Thus, it was not possible to make a reflection measurement in which the electric field was everywhere parallel to the optic axis.

For the transmission measurements of  $\text{BaTiO}_3$ , thin samples a few microns thick were produced by continued etching in hot  $\text{H}_3\text{PO}_4$  slightly above the Curie temperature ( $120^\circ\text{C}$ ) as described by Last.<sup>19</sup> After etching, the samples were dc poled in water to produce entirely  $c$ -domained plates. The thickness was calculated from

<sup>18</sup> P. H. Fang, Phys. Rev. **108**, 242 (1957).

<sup>19</sup> J. T. Last, Rev. Sci. Instr. **28**, 720 (1957).

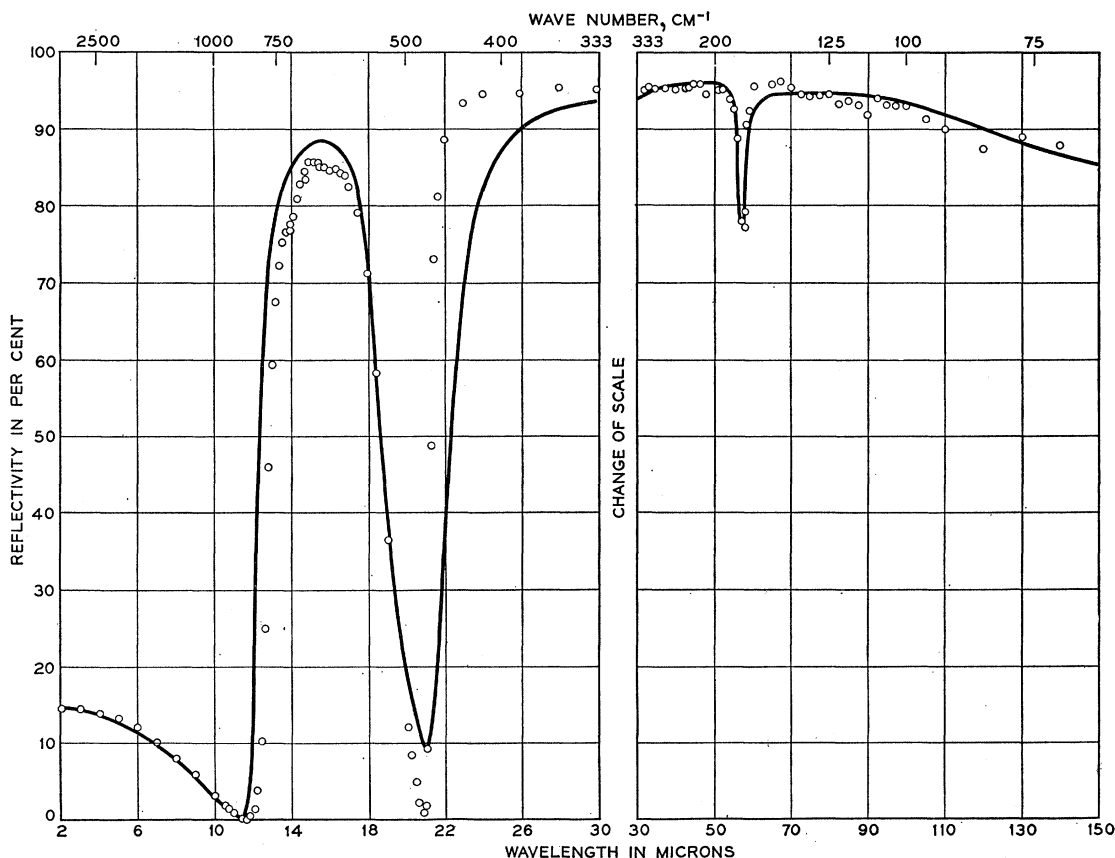


FIG. 3. Reflectivity of  $\text{SrTiO}_3$ . The curve was calculated by using dispersion theory.

observations of the width of  $a$  domains before dc poling, and from dial gauge measurements.

$\text{SrTiO}_3$  samples were cut from an undoped boule grown by flame fusion and one surface polished by using normal optical-polishing techniques. Since  $\text{SrTiO}_3$  has cubic symmetry, the orientation of the sample faces with respect to the crystal lattice was not determined.

With one exception, the rutile samples were obtained from either of two x-ray orientated undoped boules grown by flame fusion. The one exception was a natural crystal. Again, the usual optical polishing methods were employed to prepare the surfaces to be measured.

#### EXPERIMENTAL RESULTS

Room-temperature normal-incidence reflectivity and transmission measurements between  $5000$  and  $333\text{ cm}^{-1}$  were made by using a double-pass prism spectrometer with NaCl and CsBr prisms. Experimental techniques employed here have been previously described in detail.<sup>14</sup> For frequencies below  $333\text{ cm}^{-1}$  a single-pass grating monochromator<sup>20</sup> was used.

The measured reflectivity  $R$  of  $\text{BaTiO}_3$  for the electric

vector perpendicular to the optic axis (ordinary ray) is shown in Fig. 1 by the open circles. The wavelength scale<sup>21</sup> has been divided into the spectral range covered by each instrument. Since the samples were prepared with the optic axis normal to the surface, it was not necessary to polarize the spectrometer beam. The sample which contained approximately 50%  $a$  domains was measured with the electric vector in the beam polarized parallel to the optic axis (extraordinary ray) in the surface. The results of this measurement are shown by the dots in Fig. 1. The beam was polarized by using a stack of AgCl plates set at the polarizing angle. Since the spectrometer partially polarizes the beam, the polarizer was oriented so as to give the maximum degree of polarization. The degree of polarization obtained with this arrangement has been discussed previously.<sup>14</sup> The data points of Fig. 2 show the ordinary ray transmission of a  $(5.0 \pm 0.5)\mu$  thick single crystal of  $\text{BaTiO}_3$ . For comparison, the dashed curve of Fig. 2 gives the measured transmission of powdered  $\text{BaTiO}_3$  (grain size of the order of  $1\mu$ ) in a KBr pellet. Since KBr does not have

<sup>20</sup> H. W. Marshall and K. Miklus, oral presentation at Columbus Symposium on Molecular Structure and Spectroscopy, Ohio State University, Columbus, Ohio, June 19, 1958. (Copies available from Perkin-Elmer Corporation, Norwalk, Connecticut.)

<sup>21</sup> A linear wavelength rather than wave number scale has been used to plot reflectivity and transmission data in order to avoid expanding the relatively uninteresting short wavelength data. However, for convenience, several wave-number values are given at the top of the figures.

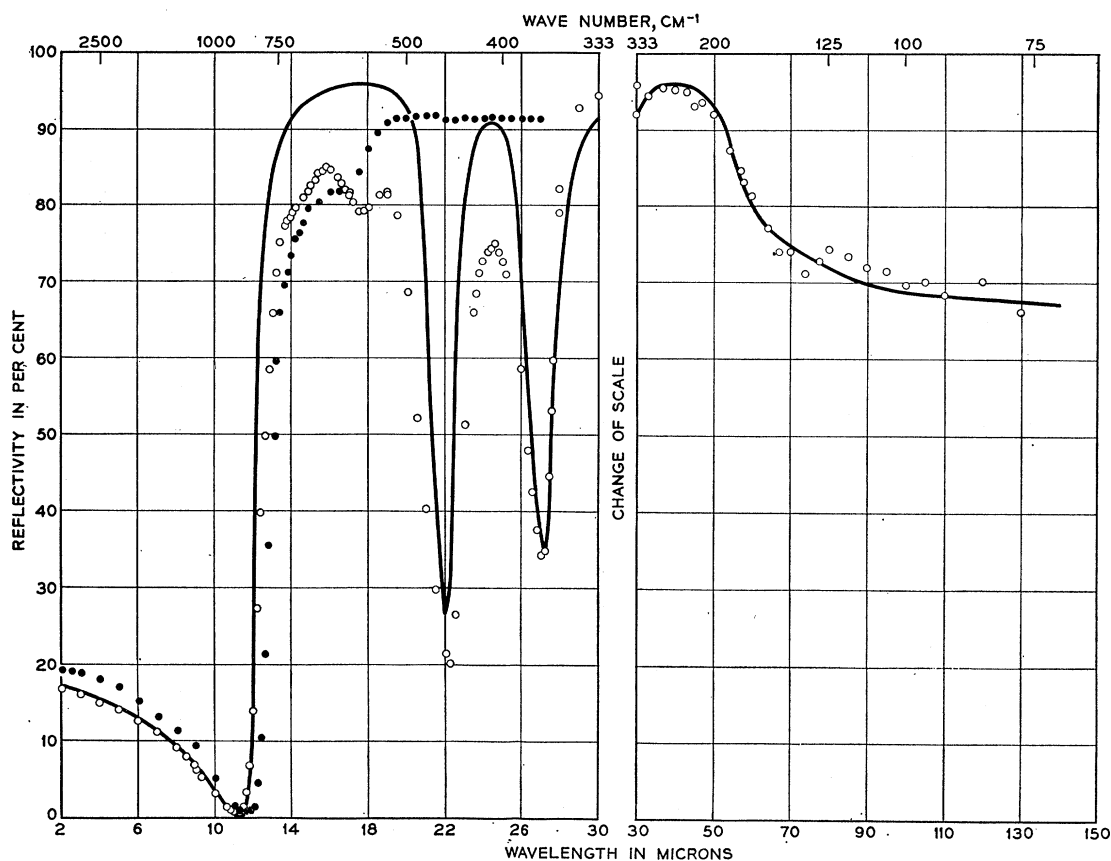


FIG. 4. Reflectivity of  $\text{TiO}_2$  for both the ordinary ray (open circles) and extraordinary ray (dots). The curve was calculated by using dispersion theory.

absorption bands in the spectral range shown, any structure observed will be due to absorption or scattering by the  $\text{BaTiO}_3$  powder.

The points in Figs. 3 and 4 give the reflectivity of  $\text{SrTiO}_3$  and  $\text{TiO}_2$ , respectively. In the latter case, the reflectivity for both the ordinary (open circles) and the extraordinary rays are plotted. However, because of the unexpected nature of the results for the synthetic  $\text{TiO}_2$  crystals, which will be discussed presently, the data were compared with measurements of a natural crystal. Due to the sample geometry, only the reflectivity for the ordinary ray was measured. This natural crystal had a reflectivity which agreed very well with that of the synthetic material.

#### ANALYSIS OF DATA

Recently, it has become common practice to analyze reflectivity data, such as that shown in Figs. 1, 3, and 4, by using a Kramers-Kronig relation.<sup>14</sup> The K-K relation used for the reflectivity  $R$  may be written as

$$\theta(\nu) = \frac{2\nu}{\pi} \int_0^{\infty} \frac{\ln r(\nu')}{\nu'^2 - \nu^2} d\nu', \quad (1)$$

where the reflectivity amplitude is  $re^{i\theta}$ , and  $r = R^{\frac{1}{2}}$ . The

real and imaginary parts of the complex dielectric constant,  $\epsilon'$  and  $\epsilon''$ , respectively, can be obtained from the relations

$$\epsilon' = n^2 - k^2, \quad (2)$$

$$\epsilon'' = 2nk, \quad (3)$$

and

$$re^{i\theta} = \frac{[(n-1) - ik]}{[(n+1) - ik]}, \quad (4)$$

where  $n$  is the refractive index and  $k$  the extinction coefficient. The machine program used to calculate  $\epsilon'$  and  $\epsilon''$  is an only slightly modified version of one described in an earlier study.<sup>14</sup> Previously, the infinite integral in Eq. (1) was approximated by a finite integral over the range of the available data plus a correction term. The integral was evaluated by representing  $\ln r(\nu')$  by straight line segments between data points. In the present program, the necessity of using a correction term was eliminated by extrapolating the data to cover the infinite interval of Eq. (1). This extension of the data was accomplished by including the limiting values of  $R$  predicted from known values of the high- and low-frequency dielectric constants. It is assumed that  $k \ll n$  at these limiting frequencies so that

$$R = (\epsilon^{\frac{1}{2}} - 1)^2 / (\epsilon^{\frac{1}{2}} + 1)^2. \quad (5)$$

TABLE I. Limiting values of the dielectric constants used in the K-K analyses.

	BaTiO <sub>3</sub>	Refer- ence <sup>a</sup>	SrTiO <sub>3</sub>	Refer- ence <sup>a</sup>	TiO <sub>2</sub>	Refer- ence <sup>a</sup>
$\epsilon_0$	2000	3, 4	310	6	89	2
$\epsilon_\infty$	5.29	22	5.20	23	6.00	24

<sup>a</sup> The reflectivity measurements at short wavelengths and the data given in these references were both considered in determining the values of  $\epsilon_\infty$ .

Since the materials considered here are transparent in the visible and known to have loss tangents,  $\epsilon''/\epsilon'$ , small compared to unity in the microwave region, the assumption that  $k \ll n$  is a reasonable one. The values for  $\epsilon_\infty$  and  $\epsilon_0$  used here are listed in Table I.<sup>2-4, 6, 22-24</sup>

A second method<sup>14</sup> used for many years to study reflectivity data, such as that obtained here, is to approximate the crystal as a system of damped oscillators having an appropriate frequency and dipole moment. This method is usually referred to as classical dispersion analysis. In recent years, with the advent of machine calculations, a number of materials have been successfully studied in this way.<sup>25</sup> The measured reflection spectra have been quantitatively fitted. Most of these cases were for isotropic diatomic crystals in which there is only one optically active resonance frequency. However, it was recently demonstrated for quartz<sup>14</sup> that classical dispersion analysis could correctly reproduce a quite complicated lattice band spectrum. An accurate dispersion analysis has not been attempted for materials with large values of  $\epsilon_0$ , such as are being considered here. There has been reported in the literature one attempt to make a qualitative fit for the ordinary ray reflectivity for rutile.<sup>9</sup>

According to dispersion theory,  $\epsilon'$  and  $\epsilon''$  as functions of frequency are given by

$$\epsilon'(\nu) = n^2 - k^2 = \epsilon_\infty + \sum_i \frac{4\pi\rho_j\nu_j^2}{(\nu_j^2 - \nu^2)^2 + \gamma_j^2\nu^2} \quad (6)$$

and

$$\epsilon''(\nu) = 2nk = \sum_i \frac{4\pi\rho_j\nu_j^2\gamma_j\nu}{(\nu_j^2 - \nu^2)^2 + \gamma_j^2\nu^2}, \quad (7)$$

where the summation is over the  $j$  resonances in the spectrum. Each resonance is characterized by its dispersion parameters which are the strength  $4\pi\rho_j$ , width  $\gamma_j$ , and resonance frequency  $\nu_j$ . Here, as in the previously described calculations, it is assumed that  $\gamma_j$  is independent of  $\nu$ . The normal incidence reflectivity is given by

$$R = [(n-1)^2 + k^2] / [(n+1)^2 + k^2]. \quad (8)$$

<sup>22</sup> G. Busch, H. Flury, and W. Merz, *Helv. Phys. Acta.* **21**, 212 (1948).

<sup>23</sup> S. B. Levin, N. J. Field, F. M. Pluck, and L. Merker, *J. Opt. Soc. Am.* **45**, 737 (1955).

<sup>24</sup> J. R. DeVore, *J. Opt. Soc. Am.* **41**, 416 (1951).

<sup>25</sup> W. G. Spitzer, D. Kleinman, and D. Walsh, *Phys. Rev.* **113**, 127 (1959); W. G. Spitzer, D. Kleinman, and C. J. Frosch, *ibid.* **113**, 133 (1959); R. J. Collins and D. Kleinman, *J. Phys. Chem. Solids*, **11**, 190 (1959); D. A. Kleinman and W. G. Spitzer, *Phys. Rev.* **118**, 110 (1960).

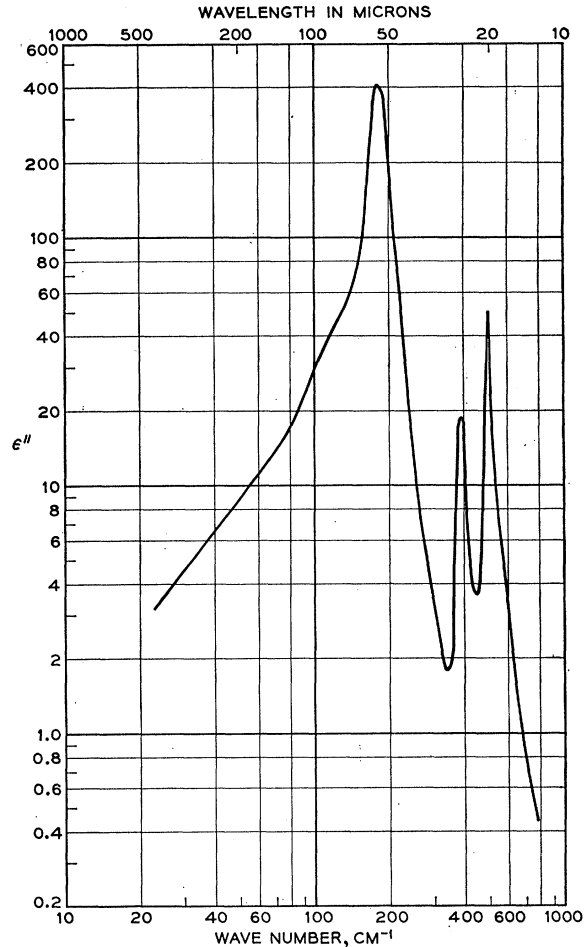


Fig. 5. Imaginary part of the dielectric constant of TiO<sub>2</sub> for the ordinary ray calculated from the data given in Fig. 4.

The trial and adjustment process generally used to obtain a fit between the dispersion calculation and experimental data has already been discussed in considerable detail.<sup>14</sup> In the present case, however, dispersion parameters are obtained directly from the K-K analysis. Each peak in the plot of  $\epsilon''$  vs energy provided by the K-K analysis represents a resonance. From the detailed characteristics of these peaks, dispersion parameters  $\nu_j$ ,  $\gamma_j$ , and  $4\pi\rho_j$  were calculated for each resonance. The frequency of a given resonance is the frequency at which the conductivity  $\sigma$ ,

$$\sigma_j = \epsilon_j''\nu/2, \quad (9)$$

is a maximum.<sup>26</sup> The quantity  $\epsilon_j''$  is the contribution of the  $j$ th resonance to  $\epsilon''$ . In the approximation  $\gamma_j/\nu_j \ll 1$ , the maximum of  $\epsilon_j''$  also occurs at  $\nu_j$ .

For the calculation of  $\gamma$ , two cases must be considered. If  $\gamma_j/\nu_j \ll 1$ , then  $\gamma$  is given by the frequency half-width of the  $\epsilon''$  peak. For  $\gamma_j/\nu_j$  of the order of unity or larger,

<sup>26</sup> F. Seitz, *Modern Theory of Solids* (McGraw-Hill Book Company, Inc., New York, 1940), Chap. XVII, p. 635.

TABLE II. Dispersion parameters calculated from the K-K analyses.<sup>a</sup>

	BaTiO <sub>3</sub> Ordinary ray	SrTiO <sub>3</sub>	TiO <sub>2</sub> Ordinary ray
$\lambda_1, \nu_1$	20.4 $\mu$ , 491 cm <sup>-1</sup>	18.4 $\mu$ , 544 cm <sup>-1</sup>	20.0 $\mu$ , 500 cm <sup>-1</sup>
$\gamma_1/\nu_1$	0.059±0.002	0.049±0.002	0.044±0.004
$4\pi\rho_1$	0.60±0.03	1.56±0.06	2.0±0.2
$\gamma_2, \nu_2$	54.8 $\mu$ , 183 cm <sup>-1</sup>	(56.3±0.5) $\mu$ , (178±2.0) cm <sup>-1</sup>	25.8 $\mu$ , 388 cm <sup>-1</sup>
$\gamma_2/\nu_2$	0.030±0.006	0.039±0.004	0.058±0.006
$4\pi\rho_2$	2.2±0.4	3.6±0.4	1.08±0.1
$\lambda_3, \nu_3$	(296±8) $\mu$ , (33.8±0.9) cm <sup>-1</sup>	(114.3±1.1) $\mu$ , (87.7±0.9) cm <sup>-1</sup>	(54.8±0.5) $\mu$ , (183±1.8) cm <sup>-1</sup>
$\gamma_3/\nu_3$	2.5±0.1	0.5±0.1	0.19±0.01
$4\pi\rho_3$	1830±70	311±62	81.5±4.1

<sup>a</sup> The uncertainties quoted here are those estimated from the uncertainties encountered in obtaining the various quantities from the plots of  $\epsilon''$  and  $\sigma$  vs energy. Therefore they are simply lower limits on the reliability of the figures given.

the frequency half-width of  $\epsilon''$  is no longer equal to  $\gamma_j$ ; and in addition, the frequency at which  $\epsilon''$  reaches its maximum is not equal to  $\nu_j$ . This latter fact, i.e., the difference in frequencies between the maxima of  $\sigma$  and  $\epsilon''$ , has been used to determine  $\gamma$ . The maximum of  $\epsilon_j''$  occurs at frequency  $\nu_j'$  given by

$$(\nu_j')^2 = \frac{\nu_j^2}{6} \left( 2 - \frac{\gamma_j}{\nu_j} \right) \left[ 16 - 4 \left( \frac{\gamma_j}{\nu_j} \right)^2 + \left( \frac{\gamma_j}{\nu_j} \right)^4 \right]^{-\frac{1}{2}}. \quad (10)$$

A graphical solution of Eq. (10) has been used to obtain  $\gamma_j$  from determinations of  $\nu_j'$  and  $\nu_j$ .

The strength of the resonance is determined from the maximum of  $\sigma_j$ ,  $\sigma_j^{\max}$ , where

$$4\pi\rho_j = 2\gamma_j\sigma_j^{\max}/\nu_j^2. \quad (11)$$

Assuming a reflectivity curve is capable of being fitted by classical dispersion theory, the accuracy of the above procedure for obtaining the dispersion parameters has been tested in the following manner: An arbitrary  $\epsilon_\infty$  and a set of dispersion parameters  $\nu_1=100$  cm<sup>-1</sup>,  $4\pi\rho=500$ , and  $\gamma/\nu_1=1.00$  were used to calculate an exact reflectivity curve. The K-K analysis of the reflectivity curve was then used to obtain the dispersion parameters which were  $\nu_1=100\pm 1.0$  cm<sup>-1</sup>,  $4\pi\rho=496\pm 20$ , and  $\gamma/\nu_1=1.02\pm 0.04$  in good agreement with the assumed values.

## RESULTS OF ANALYSES

Since the K-K analysis for rutile is the simplest to discuss, the results for this material will be presented first. The  $\epsilon''(\nu)$  curve obtained from the K-K analysis of the ordinary ray data of Fig. 4 is given in Fig. 5. At the lowest measured frequency, the reflectivity is close to the limiting value of  $R_0=0.655$  corresponding to  $\epsilon_0=89$ .<sup>2</sup> The  $\epsilon''$  indicates that three resonances occur all well within the measured frequency range. Therefore, the nature of the extrapolation of  $R$  to the low-frequency value  $R_0$  has very little effect on the analysis, i.e.,  $\epsilon''(\nu)$  is small in the extrapolated region. The strength and width of the lowest frequency resonance are clearly much greater than that of the two higher frequency resonances. The dispersion parameters calculated from

the K-K analysis are given in Table II. The extraordinary ray reflectivity measurements for rutile do not cover a wide enough spectral range to allow an accurate K-K analysis. However, it is clear from the reflectivity measurements of Fig. 4 that the experimental data are compatible with one main resonance.

The K-K plot of  $\epsilon''$  for SrTiO<sub>3</sub> is given in Fig. 6 and the calculated dispersion parameters are listed in Table II. The  $\epsilon_\infty + \sum_j 4\pi\rho_j \approx 310$  which is the correct value for  $\epsilon_0$ . Therefore, it is not necessary to assume any resonance with  $\nu_j < 70$  cm<sup>-1</sup> in order to explain the data. The experimental data of Fig. 3 which end at  $\approx 70$  cm<sup>-1</sup> are still larger than the limiting value of  $R_0=0.797$  corresponding to  $\epsilon_0=310$ . The  $\epsilon''$  curve of Fig. 6 was obtained by assuming a linear extrapolation of  $R$  from the lowest measured frequency to  $R=0.797$  at  $\nu \leq 10$  cm<sup>-1</sup>. The effect of this assumption was checked by recalculating  $\epsilon''$  when we extrapolated linearly to  $R=0.797$  at  $\nu \leq 0.7$  cm<sup>-1</sup>. The value  $\nu=0.7$  cm<sup>-1</sup> corresponds to a frequency region where  $\epsilon_0=310$  has been measured.<sup>6</sup> For  $\nu \geq 70$  cm<sup>-1</sup> the  $\epsilon''$  calculated for each of the above extrapolations showed very little difference. The three peaks were all at the same frequencies and the value of  $\epsilon''$  agreed everywhere within 10%. Because of the localizing effect of the  $1/(\nu'^2 - \nu^2)$  term in Eq. (1), the nature of the extrapolation would be expected to have a much stronger effect on the  $\epsilon''$  values for  $\nu \leq 70$  cm<sup>-1</sup>, and therefore  $\epsilon''$  for this spectral range is not given in Fig. 6.

Of the three materials, the K-K analysis of the ordinary ray reflectivity for BaTiO<sub>3</sub> presents the greatest difficulty. The general features of the lattice spectrum are quite similar to those for SrTiO<sub>3</sub>, as one would have guessed from the marked similarity of the reflectivity data. The main difference between the BaTiO<sub>3</sub> and the other two materials is that the lowest frequency resonance is beyond the measured frequency range. Therefore the shape and peak position of  $\epsilon''$  for this resonance is going to be sensitive to the extrapolation of  $R$ . Figure 7 shows the  $\epsilon''$  curve, where the  $R$  has been linearly extrapolated from  $\nu=70$  cm<sup>-1</sup> to a value  $R_0=0.914$  at  $\nu \leq 1.87$  cm<sup>-1</sup>. The  $R_0$  value assumes  $\epsilon_0=2000$ , and

$\nu = 1.87 \text{ cm}^{-1}$  corresponds to 56 kMc/sec where this value of  $\epsilon_0$  has been measured.<sup>4</sup> The dispersion parameters are listed in Table II. A second calculation was done where  $R$  was linearly extrapolated to  $R_0$  at  $\nu \leq 20 \text{ cm}^{-1}$ . As in the  $\text{SrTiO}_3$  case, the two extrapolations gave nearly identical results for  $\nu > 70 \text{ cm}^{-1}$ , however, the  $\nu_3 = 33.8 \text{ cm}^{-1}$  of Table II changed to  $27.0 \text{ cm}^{-1}$  for the second case. In the latter case, it should be pointed out that with a resonance at  $27 \text{ cm}^{-1}$  it is not reasonable to expect  $R = R_0$  at  $20 \text{ cm}^{-1}$ . This conclusion is supported by the dispersion analysis which gives an exceptionally poor fit to the data throughout the entire spectral region when the dispersion parameters of the K-K analysis from the second extrapolation are used. While we are unable to assign the inaccuracy of the  $\nu_3 = 33.8 \text{ cm}^{-1}$  figure, it is felt that the K-K analysis indicates that the resonance is placed in the proper frequency range. Further justification for a  $\nu_3$  close to  $33.8 \text{ cm}^{-1}$  will be

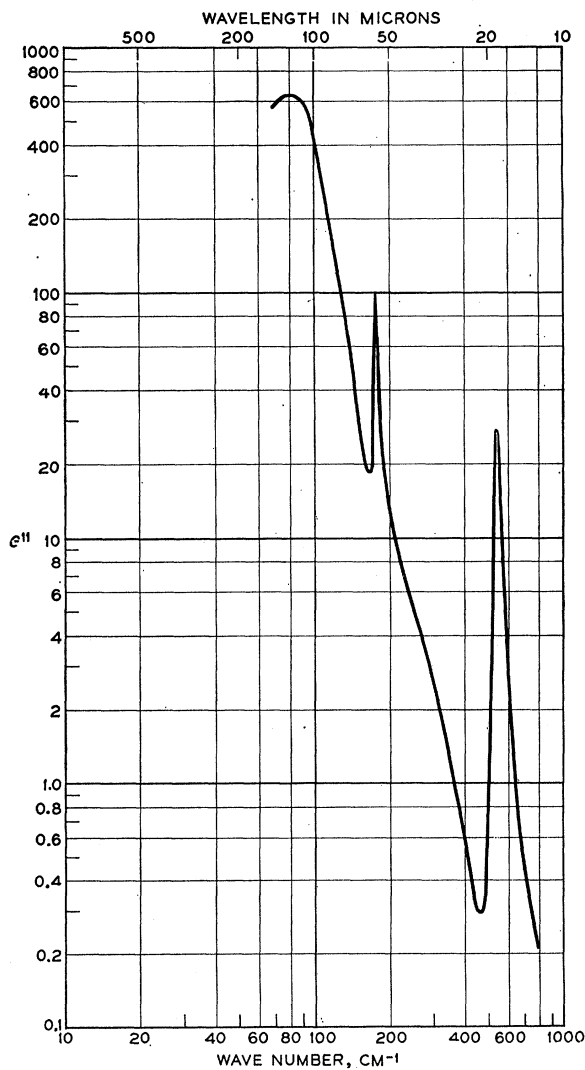


FIG. 6. Imaginary part of the dielectric constant of  $\text{SrTiO}_3$  obtained from the data in Fig. 3.

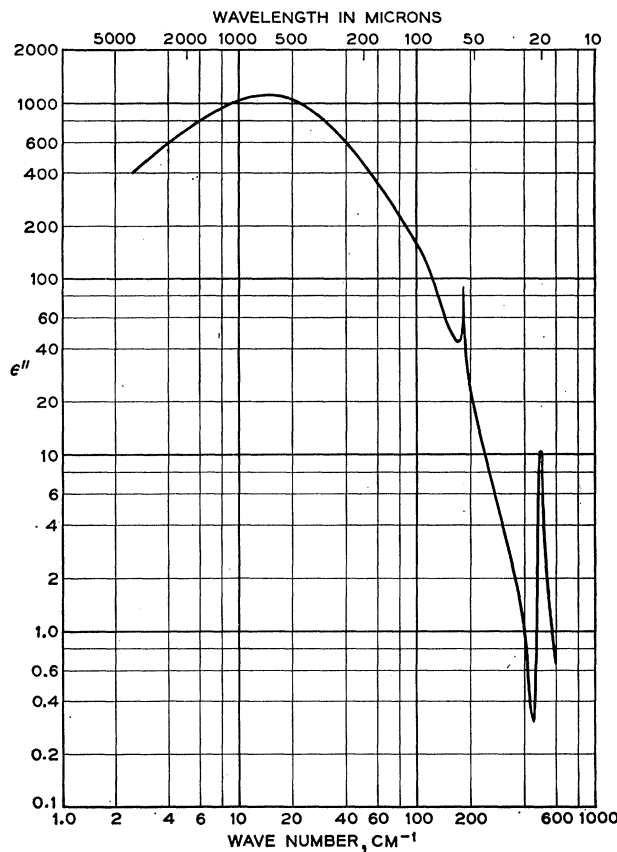


FIG. 7. Imaginary part of the dielectric constant of  $\text{BaTiO}_3$  for the ordinary ray obtained from the data given in Fig. 1.

given when the dispersion analysis is discussed. Only the ordinary ray has been studied since a pure extraordinary reflectivity spectrum was not obtained.

In none of the cases considered here do the dispersion parameters of Table II when used in Eqs. (6)–(8), give reflectivity curves in precise agreement with the data. While minor improvements in the calculated curves could be produced by adjustments in the dispersion parameters, the data still could not be fitted accurately. The calculated reflectivity curves of best fit obtained to date are shown in Figs. 1, 3, and 4. The dispersion parameters for these curves are listed in Table III. In previous dispersion analyses on materials of  $\epsilon_0 \leq 10$ , the calculated curves fitted the data within the experimental accuracy of the data. However, in those cases the transition region was  $\approx \nu_j/3$  while for the present materials the transition range is as large as  $20 \nu_j$ . Therefore, assuming  $\gamma_3$  to be frequency independent is a much more drastic assumption in the present study than in those previously cited. One of the major difficulties in obtaining accurate fits with the dispersion calculations in each case arises from the large value of  $\gamma_3$ , which must be used in order to keep the calculated reflectivity from rising above the measured value in the long-wavelength region. With this large  $\gamma_3$ , the sharpness of the structure

TABLE III. Dispersion parameters for the best fit to the reflectivity data.

	BaTiO <sub>3</sub> Ordinary ray	SrTiO <sub>3</sub>	TiO <sub>2</sub> Ordinary ray	TiO <sub>2</sub> Extraordinary ray
$\lambda_1, \nu_1$	19.6 $\mu$ , 510 cm <sup>-1</sup>	18.2 $\mu$ , 546 cm <sup>-1</sup>	20.9 $\mu$ , 479 cm <sup>-1</sup>	
$\gamma_1/\nu_1$	0.057	0.049	0.025	
$4\pi\rho_1$	1.0	1.9	2.0	
$\lambda_2, \nu_2$	54.7 $\mu$ , 183 cm <sup>-1</sup>	56.3 $\mu$ , 178 cm <sup>-1</sup>	25.9 $\mu$ , 386 cm <sup>-1</sup>	
$\gamma_2/\nu_2$	0.031	0.034	0.03	
$4\pi\rho_2$	2.0	3.6	2.0	
$\lambda_3, \nu_3$	296 $\mu$ , 33.8 cm <sup>-1</sup>	114.3 $\mu$ , 87.5 cm <sup>-1</sup>	52.5 $\mu$ , 189 cm <sup>-1</sup>	52.5 $\mu$ , 189 cm <sup>-1</sup>
$\gamma_3/\nu_3$	2.5	0.3	0.1	
$4\pi\rho_3$	2000	299.3	78.5	

at shorter wavelengths could not be reproduced. This difficulty is most clearly seen in Fig. 1 where a large discrepancy occurs between the calculated curve and the data in the range from 22 to 28  $\mu$ . It therefore appears necessary to allow  $\gamma_3$  to be frequency dependent before a satisfactory fit to the data can be accomplished. This conclusion is consistent with the recent report of a dispersion analysis study<sup>27</sup> of LiF, NaCl, and CsBr, where it was also found necessary to assume a frequency-dependent damping constant.

The position of the main resonance in TiO<sub>2</sub> for the extraordinary ray can be estimated from the dispersion equations. When  $\nu_m$  is the frequency of the reflectivity minimum in Fig. 4 then for a single resonance Eq. (6) becomes

$$1 - \epsilon_\infty = \frac{4\pi\rho}{1 - (\nu_m/\nu_1)^2}, \quad (12)$$

where  $\nu_1$  is the resonance frequency. It has been assumed in Eq. (12) that  $\gamma^2\nu_m^2 \ll (\nu_1^2 - \nu_m^2)^2$ . Since at the reflectivity minimum,  $R \approx 0$ ,  $\epsilon' = 1$ . From  $\epsilon_0 = 173$  and  $\epsilon_\infty = 8.4^2$  one obtains  $4\pi\rho = 165$ . With  $\nu_m = 870$  cm<sup>-1</sup>, the resonance frequency is  $\approx 189$  cm<sup>-1</sup>. This frequency has been listed in the  $\nu_3$  row of Table III since the resonance corresponds in frequency and strength much more closely to the  $\nu_3$ , than to the  $\nu_1$  or  $\nu_2$  resonance for the ordinary ray case. The assumption that  $\gamma^2\nu_m^2 \ll (\nu_1^2 - \nu_m^2)^2$  is valid to within 10% if  $\gamma/\nu_1 < 1.4$ .

It may be noted that the reflectivity curve of the ordinary ray for BaTiO<sub>3</sub> in Fig. 1 was calculated with  $\nu_3 = 33.8$  cm<sup>-1</sup>. The calculated curve and the data are in reasonably good agreement at the reflectivity minimum near 770 cm<sup>-1</sup>. Through Eq. (12), any relative change in  $\nu_3$  will produce almost the same relative change in  $\nu_m$  if  $\epsilon_\infty$  and  $4\pi\rho$  are held constant. It is therefore concluded that  $\nu_3 = 33.8$  cm<sup>-1</sup> is close to the correct value.

#### LOSS TANGENTS IN THE MICROWAVE REGION

The contributions of the infrared absorption bands to the loss tangent,

$$\tan\delta = \epsilon''/\epsilon', \quad (13)$$

can be estimated from the dispersion parameters. The frequencies which will be considered here are in the microwave region where experimental data are available. In this frequency range the only significant contribution to  $\epsilon''$  will be that due to the broad low-frequency resonance. For the three materials studied, at least 90% of  $\epsilon''$  arises from the strength of this same resonance so that if dispersion theory is assumed, Eq. (13) can be approximated to within at least 10% by

$$\tan\delta \approx \gamma_3\nu/\nu_3^2(1 - \nu^2/\nu_3^2) \approx \gamma_3\nu/\nu_3^2. \quad (14)$$

Equation (14) is now the contribution to the loss tangent at frequency  $\nu$  due to a resonance of width  $\gamma_3$  at frequency  $\nu_3$ . Note that the strength of the resonance does not appear directly in Eq. (14) and also that the loss tangent increases with frequency at least as fast as  $\nu$ .

The values of  $\tan\delta$  calculated from Eq. (14) are given in Table IV<sup>2,3,5,28</sup> for frequencies at which there are room temperature experimental microwave data. The loss tangents have been calculated from the dispersion parameters obtained from the K-K analyses (Table II) and also from the dispersion parameters which give the best fit to the experimental reflectivity data (Table III). The experimental and calculated values of  $\tan\delta$  are in reasonable agreement. Of particular interest are the loss tangents of BaTiO<sub>3</sub> which microwave measurements have shown to be anomalously large. The calculated values for BaTiO<sub>3</sub> indicate that, at room temperature, single crystals of this material are inherently lossy in the microwave region for the ordinary ray. Experimental data on SrTiO<sub>3</sub> at  $-110^\circ\text{C}$  show that the loss tangent increases linearly with frequency in the measured range

TABLE IV. Experimental and calculated microwave loss tangents.

	Frequency (kMc/sec)	Exper.	Reference	K-K analysis	Best dis- persion fit
BaTiO <sub>3</sub>	24	$1.2 \times 10^{-1}$	3	$0.6 \times 10^{-1}$	$0.6 \times 10^{-1}$
BaTiO <sub>3</sub>	56	$1.3 \times 10^{-1}$	28	$1.4 \times 10^{-1}$	$1.4 \times 10^{-1}$
SrTiO <sub>3</sub>	22	$1.5 \times 10^{-3}$	5	$4.2 \times 10^{-3}$	$2.5 \times 10^{-3}$
TiO <sub>2</sub>	3	$3 \times 10^{-4}$	2	$3.7 \times 10^{-4}$	$1.8 \times 10^{-4}$

<sup>27</sup> H. Biltz, L. Genzel, and H. Happ, Z. Physik **160**, 535 (1960).

<sup>28</sup> R. F. Trambarulo (private communication).

from about 3 kMc/sec to 36 kMc/sec.<sup>29</sup> This observed frequency dependence is in agreement with Eq. (14). The estimates of  $\tan\delta$  given here provide lower limits for the loss tangent, since other mechanisms may also contribute microwave losses.

### DISCUSSION

In the present measurements of BaTiO<sub>3</sub> and SrTiO<sub>3</sub>, all three predicted<sup>7</sup> infrared active resonances have been observed. From Table II the three resonances in BaTiO<sub>3</sub> (ordinary ray) are at 491, 183, and 33.8 cm<sup>-1</sup>; and in SrTiO<sub>3</sub> they are at 544, 178, and 87.7 cm<sup>-1</sup>. In each case, the two high-frequency resonances have strengths of the order of unity, similar to that found in a number of ionic crystals. However, the lowest frequency resonance for each has an extremely large  $4\pi\rho$  value and accounts for the large low-frequency dielectric constant. As predicted by the theories of Anderson<sup>12</sup> and Cochran,<sup>13</sup> the large low-frequency dielectric constant is accounted for by a single low-frequency optical mode of vibration. It is also interesting to note that the low-frequency mode in BaTiO<sub>3</sub> is overdamped, i.e.,  $\gamma_3/\nu_3 > 2$ , as suggested by Landauer.<sup>13</sup>

The present reflectivity data for the titanates are in good agreement with those of Last<sup>7</sup> (1000 to 400 cm<sup>-1</sup>) except for the frequency range immediately following the first reflectivity minimum where somewhat higher values are obtained here. Last also made transmission measurements of thin BaTiO<sub>3</sub> crystals and powder—KBr pellets for both BaTiO<sub>3</sub> and SrTiO<sub>3</sub>. On the basis of these measurements, it was concluded that two of the fundamental absorption bands in each material had been observed: the first near 600–500 cm<sup>-1</sup>, and the second near 400–350 cm<sup>-1</sup>. It should be emphasized that the evidence for the lower frequency resonance in both titanates was based solely on the pellet measurements. Last has considered the vibrational nature of the TiO<sub>3</sub> group by discussing the symmetry properties of a central Ti atom octahedrally surrounded by six O atoms. He concludes that cubic BaTiO<sub>3</sub> and SrTiO<sub>3</sub> each have three triply degenerate infrared-active vibrations. The three normal modes proposed by Last are a Ti-O stretching mode, a Ti-O bending mode, and a cation-(TiO<sub>3</sub>) mode. Following customary procedures, the highest frequency mode was assumed to be the Ti-O stretching vibration, while the lowest, which Last believed was beyond his measured frequency range, was the cation-(TiO<sub>3</sub>) vibration. Last estimated the position of the cation-(TiO<sub>3</sub>) mode from specific heat data to be  $\approx 225$  cm<sup>-1</sup>.

The higher-frequency mode measured by Last is in reasonable agreement with the present results. However, none of the titanate resonances proposed here from either the K-K analysis or the classical dispersion calculations occur near  $\nu=400$ –350 cm<sup>-1</sup> where Last places the Ti-O bending mode. It is this mode which was

proposed exclusively on the basis of KBr pellet measurements such as that shown by the dashed curve of Fig. 2. The presence of a strong resonance here would be puzzling, since all three active modes have already been observed. As a further check on the possible existence of a strong absorption band in the above frequency range, the transmission of a  $(5.0 \pm 0.5)$   $\mu$  thick BaTiO<sub>3</sub> sample was measured (Fig. 2). The transmission was also calculated from the optical constants,  $n$  and  $k$ , deduced from the K-K analysis and the standard thin-film transmission formula.<sup>30</sup> It was found that good agreement between the measured and calculated transmissions could be obtained if a thickness of 4.5  $\mu$  was assumed. The result of the calculation is shown by the solid curve in Fig. 2. The agreement indicates that the optical constants obtained from the K-K analysis are reasonable, and an additional resonance is not needed to explain the observed transmission. Furthermore, neither the experimental data nor the calculated curve for the thin sample show the rise in transmission at the lower frequencies as observed in the pellet. Therefore, one is forced to conclude that the minimum in transmission near  $\nu=400$ –350 cm<sup>-1</sup> for the titanate-KBr pellet is not due to an absorption band. The low-frequency behavior in the pellet's transmission might be a scattering effect as also suggested by BT.<sup>15</sup>

Barker and Tinkham<sup>15</sup> have extended the reflectivity measurements on SrTiO<sub>3</sub> to the very far infrared (2.5 cm<sup>-1</sup>). They have analyzed their data using a K-K relation and find only two  $\epsilon''$  peaks, near 550 and 100 cm<sup>-1</sup>, as compared to the corresponding peaks of Fig. 6 at 543 and 82 cm<sup>-1</sup>. However, the most important difference between the two pieces of work is the narrow resonance at 178 cm<sup>-1</sup> observed here and not reported by BT. (*Note added in proof.* In a recent communication from Dr. Barker we have been informed that he has also observed the 178 cm<sup>-1</sup> band in SrTiO<sub>3</sub>.) The position of BT's higher frequency resonance is in excellent agreement with that reported here. However, the value 82 cm<sup>-1</sup> given here for the low-frequency resonance is preferred. The value of 100 cm<sup>-1</sup> given by BT for the  $\epsilon''$  peak for this resonance is not compatible with dispersion theory since calculations show that the reflectivity minimum near 11  $\mu$  shifts to less than 10  $\mu$  in disagreement with the data given here as well as that of BT. The temperature dependence of the low-frequency mode observed by BT supports the contention that the vibrational mode is responsible for the Curie point behavior of the low-frequency dielectric constant as proposed by recent theories.<sup>12,13</sup>

For the case of rutile, the present measurements show three resonances for the ordinary ray located at 500, 388, and 183 cm<sup>-1</sup>; and one resonance for the extraordinary ray at 189 cm<sup>-1</sup>. As with the titanates, the lowest frequency resonance is much stronger than those at higher frequencies and accounts for the high value of  $\epsilon_0$ .

<sup>29</sup> G. Rupprecht and R. O. Bell, Phys. Rev. **125**, 1915 (1962).

<sup>30</sup> R. B. Barnes and M. Czerny, Phys. Rev. **38**, 338 (1931).

The only previously published experimental data for the far-infrared reflectivity of rutile known to the authors are the early measurements of Liebis and Rubens.<sup>8</sup> They measured the reflectivity of natural rutile crystals for both the ordinary and extraordinary rays from 7000 to 33 cm<sup>-1</sup>. Throughout much of the experimental range our measurements are in good agreement with this data. However, between 500 and 333 cm<sup>-1</sup>, the present measurements show two strong dips in the ordinary-ray reflectivity and none for the extraordinary ray. The Liebis and Rubens data show one for each ray. It was for this reason that the synthetic crystal results for the ordinary ray were checked by also measuring a natural crystal. From group-theoretical considerations Narayanan<sup>31</sup> has pointed out that tetragonal TiO<sub>2</sub> should have four normal modes which are active in the Raman effect and four different modes which are infrared active. Of the four infrared-active modes, three should be observed with the ordinary ray and one with the extraordinary ray, in agreement with results listed in Tables II and III. Moreover, according to the theory the infrared resonances should be forbidden in the Raman effect. Comparison is difficult since some of the Raman lines are broad, however there are no sharp peaks in the Raman spectrum with frequency shifts corresponding to the infrared frequencies.

Recently a report was given on a theoretical calculation of the strengths of the infrared absorption bands in quartz.<sup>32</sup> In the comparison between theory and experiment, it was convenient to define an experimental quantity  $S_j$  given by

$$S_j = 4\pi\rho_j\nu_j^2 / (e^2/\pi\Omega m_j), \quad (15)$$

where  $\Omega$  is the unit cell volume, and  $m_j$  is the mass of the  $j$ th normal mode. In the calculations  $m_j$  was arbitrarily assigned a value of 100 amu. From a consideration of the general theory for infrared intensities, it was demonstrated that  $\rho_j \propto \nu_j^{-2}$ .  $S_j$  therefore represents a frequency independent resonance strength. The  $S_j$  values have been obtained for each of the resonances measured here and are given in Table V. In calculating  $S_j$ , the values of  $4\pi\rho_j$  and  $\nu_j$  are taken from the K-K results of Table II. In each of the materials  $S_j$  for the low-frequency resonance is the largest although the differences are not as large as in the  $4\pi\rho_j$  values. The largest value of  $S_j$  is about twice that of the largest value in quartz ( $S_j=180$ ). The significance of the  $S_j$  quantity depends upon the effective-charge model assumed for the crystal as well as on the normal modes. The magnitude of the  $S_j$  values observed here suggests that they are explicable on the basis of physically reasonable effective charge parameters.

One striking feature noted in Table V is the similarity of the low-frequency resonance values. This similarity is to be expected if the same type of normal mode is

TABLE V. Calculated values of  $S_j$ , the frequency-independent resonance strength.

$S_j$	BaTiO <sub>3</sub> (Ordinary ray)	SrTiO <sub>3</sub>	TiO <sub>2</sub> (Ordinary ray)
$S_1$	20	61	64
$S_2$	10	15	21
$S_3$	280	316	344

responsible for the very large low-frequency dielectric constant in these crystals. Since this mode occurs in all three materials, it cannot be the cation-(TiO<sub>3</sub>) vibration. The narrow  $\nu_2$  band in the titanates near 180 cm<sup>-1</sup>, which has no corresponding band in rutile, is therefore interpreted as the cation-(TiO<sub>3</sub>) resonance. This interpretation is supported by the similarity in the values of  $S_2$  given in Table V. The frequency of this band is typical for the cation-anion vibrations of ionic crystals such as NaCl. A frequency shift of 18 cm<sup>-1</sup> would be expected between the two titanates for this mode on the assumption that it consists of a rigid motion of TiO<sub>6</sub> octahedra with respect to the cation and that the same force constants apply in each case. The fact that the observed shift given in Table III (5 cm<sup>-1</sup>) is considerably smaller than 18 cm<sup>-1</sup> shows that this assumption is not valid. In order to account for the observed shift it would be necessary to consider both the distortion of the octahedra and the different force constants in a normal mode calculation.

The  $S_j$  values of Table V clearly demonstrate the difficulty with the earlier interpretation of the titanate normal modes in which the high- and low-frequency modes are viewed as stretching and bending modes of the TiO<sub>6</sub> octahedra. Strict application of this model would require the  $S_1$  values for the titanates to be nearly the same, whereas Table V shows they differ by a factor of three. Consideration of the TiO<sub>6</sub> octahedra model suggested by Last<sup>7</sup> shows that the two TiO<sub>6</sub> modes should differ greatly in strength. The stronger of the two should be identified with low-frequency mode. The weaker, to be identified with the high-frequency mode, would be expected to be sensitive to the detailed nature of the atomic motions.

#### SUMMARY

Dispersion and K-K analyses of the near and far infrared reflectivity of both BaTiO<sub>3</sub> and SrTiO<sub>3</sub> show three fundamental lattice bands which is the predicted number of optically active lattice modes. In each of the titanates, the band of greatest interest is the lowest frequency one ( $\nu_3 \approx 34$  cm<sup>-1</sup> for the ordinary ray in BaTiO<sub>3</sub> and  $\nu_3 = 88$  cm<sup>-1</sup> for SrTiO<sub>3</sub>) which accounts for the large change with frequency in dielectric constant that occurs in these crystals. The width of the low-frequency resonances ( $\gamma_3/\nu_3$  of the order of unity) are considerably larger than those usually encountered. Significant differences between the present results and

<sup>31</sup> P. S. Narayanan, Indian Acad. Sci. **32A**, 279 (1950).

<sup>32</sup> D. A. Kleinman and W. G. Spitzer, Phys. Rev. **125**, 16 (1962).

other relevant investigations of these materials are discussed.

The analyses of the infrared reflectivity data for natural and synthetic rutile show three resonances for the ordinary ray. Limited data for the extraordinary ray are compatible with a single resonance. These results are in disagreement with the very early data for natural rutile, but they are in agreement with group theoretical predictions. As with the titanates, the strongest resonance, i.e., the one associated with the large low-frequency dielectric constant, is at the lowest frequency,  $\nu_3 \approx 185 \text{ cm}^{-1}$ , and has a width  $\gamma_3/\nu_3$  of the order of 0.1.

For all three materials investigated, attempts to fit the reflectivity data with classical dispersion theory by using three resonances were not completely satisfactory. The sharp rise with increasing wavelength in the measured reflectivity that occurs somewhere between 20 and  $30 \mu$  was not reproduced in any of the calculated curves. These analyses suggest that a frequency-dependent damping constant for  $\gamma_3$  is required to fit the experimental data accurately.

Microwave loss tangents estimated from dispersion parameters calculated from K-K as well as dispersion

analyses are in agreement with the experimentally measured quantities. Of particular interest is  $\text{BaTiO}_3$  which now appears to be inherently lossy for the ordinary ray at microwave frequencies.

The three optically active vibrations in strontium and barium titanate with frequencies  $\nu_1 > \nu_2 > \nu_3$  as listed in Table III are assigned as follows:  $\nu_1$ , a  $\text{TiO}_6$  octahedra mode of low infrared strength (described by Last as a bending mode);  $\nu_2$ , a vibration of the cation with respect to the  $\text{TiO}_6$  octahedra; and  $\nu_3$ , a  $\text{TiO}_6$  octahedra stretching mode of large infrared strength (described by Last as a stretching mode). In rutile no mode assignment has been proposed except for the low-frequency  $\nu_3$  resonance which is similar to the  $\nu_3$  resonance in the titanates. The  $\nu_3$  mode is responsible for the high dielectric constant observed in these materials.

#### ACKNOWLEDGMENTS

The authors would like to take this opportunity to acknowledge the assistance of A. Savage who assisted in preparing the samples for reflectivity measurements and also to thank Dr. Barker and Dr. Tinkham for a preprint of their paper on  $\text{SrTiO}_3$ .